INTERFACE

royalsocietypublishing.org/journal/rsif

Research

Cite this article: Jung Y, Park K, Jensen KH, Kim W, Kim H-Y. 2019 A design principle of root length distribution of plants. *J. R. Soc. Interface* **16**: 20190556.
http://dx.doi.org/10.1098/rsif.2019.0556

Received: 7 August 2019
Accepted: 14 November 2019

Subject Category:
Life Sciences–Physics interface

Subject Areas:
biophysics, biomechanics, bioengineering

Keywords:
biological fluid dynamics, root length density, plant physics, flow in porous media

Authors for correspondence:
Kaare H. Jensen
e-mail: khjensen@fysik.dtu.dk
Wonjung Kim
e-mail: wonjungkim@sogang.ac.kr
Ho-Young Kim
e-mail: hyk@snu.ac.kr

Electronic supplementary material is available online https://doi.org/10.6084/m9.figshare.c.4750583.

THE ROYAL SOCIETY PUBLISHING

A design principle of root length distribution of plants

Yeonsu Jung[1], Keunhwan Park[2], Kaare H. Jensen[2], Wonjung Kim[3] and Ho-Young Kim[1]

[1]Department of Mechanical and Aerospace Engineering, Seoul National University, Seoul 08826, Korea
[2]Department of Physics, Technical University of Denmark, 2800 Kgs. Lyngby, Denmark
[3]Department of Mechanical Engineering, Sogang University, Seoul 04107, Korea

YJ, 0000-0001-7920-3844; KP, 0000-0003-1013-5382; KHJ, 0000-0003-0787-5283; WK, 0000-0002-6866-6840; H-YK, 0000-0002-6813-2398

Shaping a plant root into an ideal structure for water capture is increasingly important for sustainable agriculture in the era of global climate change. Although the current genetic engineering of crops favours deep-reaching roots, here we show that nature has apparently adopted a different strategy of shaping roots. We construct a mathematical model for optimal root length distribution by considering that plants seek maximal water uptake at the metabolic expenses of root growth. Our theory finds a logarithmic decrease of root length density with depth to be most beneficial for efficient water uptake, which is supported by biological data as well as our experiments using root-mimicking network systems. Our study provides a tool to gauge the relative performance of root networks in transgenic plants engineered to endure a water deficit. Moreover, we lay a fundamental framework for mechanical understanding and design of water-absorptive growing networks, such as medical and industrial fluid transport systems and soft robots, which grow in porous media including soils and biotissues.

1. Introduction

Human civilization is fundamentally dependent on green plants which provide a vital link between solar radiation and metabolically accessible energy. Enhancing plant yield is increasingly important in an age of continued population growth, shortage of arable land, and dramatic changes in both local weather patterns and planetary climate conditions. Intensive research over the past decades has focused on particular aspects of plant productivity, such as enhancement of photosynthetic yield and disease resilience. However, the majority of the approaches have made only limited success due to a lack of comprehension of the inherent complexity of plant physiology [1–4]. While significant advances have been made in understanding and manipulating photosynthesis of sugars in leaves, the co-limiting processes of root water uptake as surrounded by a porous medium of soil have received markedly less attention, and as a result are still poorly understood.

Plant roots supply water to compensate for water loss via transpiration in the leaves while consuming the photosynthates produced by the leaves. Insufficient water supply may cause stomata closure and thus limit carbon dioxide uptake. By developing a conduit network, plant roots can secure sufficient water from a significant volume of the adjacent soil. However, the construction of the root branch is energetically costly due not only to carbon consumption but also to the resistance against the penetration of the soil. This naturally leads the plants to seek an optimal root design for cost-effective water absorption [5–10]. The root design is thus expected to be subject to evolutionary pressures [11].

Researchers have extensively studied the optimal design for water uptake. The design parameters of the root architecture for optimal water uptake that have been investigated to date include lateral branching density [5], topology [6], root hydraulics [7–9] and branching angle [10] for efficient water

© 2019 The Author(s) Published by the Royal Society. All rights reserved.

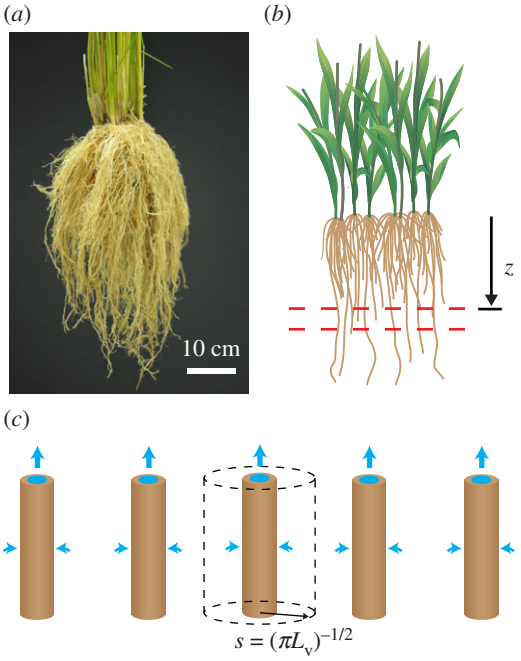

Figure 1. Plant roots. (*a*) A photograph of a rice plant (*Oryza sativa*). (*b*) A schematic illustration of the root. (*c*) Water flow in the region between the red broken lines in (*b*). Half the inter-root distance $s(z)$ is given by $s(z) = (\pi L_v)^{-1/2}$. (Online version in colour.)

acquisition. Fitter *et al*. [6] employed graph theory [12] to analyse the effects of the root topology on water uptake. Landsberg & Fowkes [7] developed a mathematical model for the minimization of the cost of water transport in xylem, thereby deducing the optimal length of a single root. Ho *et al*. [10] addressed the importance of the root branching angle considering the availability of heterogeneous soil resources including nutrients (e.g. water, nitrogen and phosphorous) and the cost of inter-root competition.

An extensive dataset of root lengths for many crops indicate that the root length density, defined as the root length per unit volume of soil decreases with depth [13,14] as shown in figures 1*a* and 2. However, the physics behind the observations have been elusive. How a root system is distributed in soil significantly influences the amount and rate of root water uptake. While the initial uptake rate in each soil layer may increase with the number of roots, the water in a highly populated layer is rapidly depleted causing a decrease in the uptake rate in the long run. A root system, thus, is forced to explore a deeper region, in which more water is available, at the expense of the high cost of construction. That is, a root system seeks a vertical distribution that can balance the benefit and cost of root construction at each soil layer, resulting in the characteristic profile over depth.

Assuming that the plant roots have evolved network structures to effectively secure water, here, we rationalize the optimal length density distribution of plant roots by considering the benefits of water uptake and the metabolic cost for a root system [15] taking over 50% of daily photosynthetic products [16,17]. It is supported by the measured root length density distributions of various plants [13,14,18,19] and by our experiments using artificial root networks. The results not only elucidate the biomechanical design principles of the root architecture but also help one to build effective fluid transport systems through porous media, such as bioscaffolds [20,21], porous reactors [22,23], filters [24,25] and soft robots [26,27].

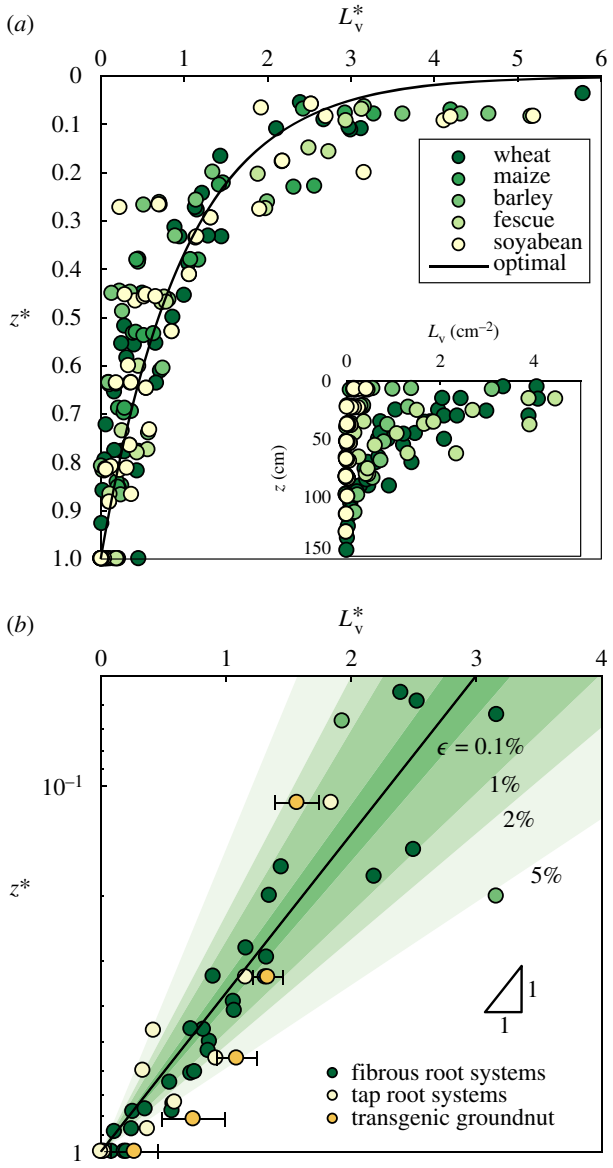

Figure 2. (*a*) Normalized root length density distribution of various plants as a function of normalized depth. The solid line corresponds to the theoretical optimum distribution. Inset: dimensional raw data of the root length density. (*b*) Comparison of normalized root length density of different types of root systems (fibrous and tap root systems, and transgenic groundnut). Normalized root length density data are plotted on a logarithmic scale in the z^*-axis. Regions of different colours correspond to the varying degree of deviation (ϵ) from the optimal curve denoted in percentage (see equation (9.1)). L_v^* of fibrous root systems lies within the 1% range. L_v^* of transgenic groundnut deviates severely (by approx. 25%) from the optimum curve especially in deep layers. The data of transgenic groundnut correspond to the average values for six different transgenic treatments with the error bar indicating the standard deviation. Data are available in electronic supplementary material, dataset S1 and references are listed in table 1 in appendix C. (Online version in colour.)

2. Root water uptake

In this article, we simplify the architecture of a real root system to one with a set of parallel root fibres having an identical diameter to that shown in figure 1*b*. This idealization is most appropriate for fibrous root systems, but can also hold for a part of tap root systems with low number of branching generations, low branching density, and uniform diameter throughout the entire root system. For root structures with

a specific purpose such as nutrient storage in tubers, the simplification may not be applied.

The vertical distribution of roots is typically quantified with the root length density [28], L_v. Figure 1*b*,*c* shows a schematic of roots with an inter-root distance of 2s at a specific depth z, so that L_v is inverse of the area [29], $L_v = 1/(\pi s^2)$. A single root with a unit length absorbs water contained in a soil volume of πs^2.

The water flux through the soil is driven by the gradient of water potential which is associated with osmosis, gravity, mechanical pressure and capillarity. For the soil partially saturated with water, the water potential gradient is known to be equivalent to the water content gradient because less water content entails the water–air interface with a higher curvature [29]. Given that the root grows mostly in the vertical direction (figure 1), the water potential gradient is assumed to be established horizontally. The local water transport in the soil around a single root element is given by the one-dimensional diffusion equation [29]

$$\frac{\partial \theta}{\partial t} = \frac{D}{r}\frac{\partial}{\partial r}\left(r\frac{\partial \theta}{\partial r}\right), \tag{2.1}$$

where $\theta(r, t)$ is the local water content at time t, D is the water diffusivity of the soil and r is the radial distance from the central line of the cylindrical root.

Equation (2.1) can be solved with the relevant initial and boundary conditions. The water potential inside the root xylem changes little during the water uptake under the assumption of a steady transpiration rate in the leaves. Owing to the relatively negligible resistance in the conduit of the root, the pressure in the root xylem remains approximately uniform. We assume that the transpiration rate during the daytime is fixed so that $\theta(r_a, t) = \theta_a$ with the constant water content, θ_a, at the entire root surface, $r = r_a$. The symmetry condition in the region between two single roots yields $\partial\theta/\partial r|_{r=0} = 0$. The initial condition is given by the initial water content of the soil θ_i, so that $\theta(r, t = 0) = \theta_i$.

Non-dimensionalizing equation (2.1) yields

$$\frac{\partial \hat{\theta}}{\partial \hat{t}} = \frac{1}{\hat{r}}\frac{\partial}{\partial \hat{r}}\left(\hat{r}\frac{\partial \hat{\theta}}{\partial \hat{r}}\right), \tag{2.2}$$

which is subject to the dimensionless initial and boundary conditions: $\hat{\theta}(\hat{r}, \hat{t} = 0) = 1$, $\hat{\theta}(\hat{r} = 1, \hat{t}) = 0$ and $\partial\hat{\theta}/\partial\hat{r}|_{\hat{r}=0} = 0$, where $\hat{\theta} = (\theta - \theta_a)/(\theta_i - \theta_a)$, $\hat{r} = (r - s)/(r_a - s)$ and $\hat{t} = Dt/(s - r_a)^2 \approx Dt/s^2$ as $s \gg r_a$. The solution of equation (2.2) is given by

$$\hat{\theta}(\hat{r}, \hat{t}) = 2\sum_{n=1}^{\infty}\frac{J_0(\lambda_n \hat{r})}{\lambda_n J_1(\lambda_n)}\exp(-\lambda_n^2\hat{t}), \tag{2.3}$$

where $J_i(r)$ is the Bessel function of the first kind with order i, and λ_n is the nth zero of $J_0(r)$.

For $\hat{t} \gg \lambda_1^{-1/2}$, the time-dependent terms with $n > 1$ vanish (e.g. $\exp(-\lambda_2^2/\lambda_1^2) \approx 0.005$) because $\exp(-\lambda_n^2\hat{t}) \ll \exp(-\lambda_n^2/\lambda_1^2) \approx 0$. Thus, $\hat{\theta}$ can be approximated as

$$\hat{\theta}(\hat{r}, \hat{t}) = \frac{2J_0(\lambda_1 \hat{r})}{\lambda_1 J_1(\lambda_1)}\exp(-\lambda_1^2\hat{t}). \tag{2.4}$$

The mean water content at time $\hat{t}$, defined as $\bar{\theta}(\hat{t}) = \int_0^1 \hat{\theta}(\hat{r}, \hat{t})\hat{r}\,d\hat{r} / \int_0^1 \hat{r}\,d\hat{r}$, is given by

$$\bar{\theta}(\hat{t}) = \sum_{n=1}^{\infty}\frac{4}{\lambda_n^2}\exp(-\lambda_n^2\hat{t}) \approx \frac{4}{\lambda_1^2}\exp(-\lambda_1^2\hat{t}). \tag{2.5}$$

Equation (2.5) implies that the mean water content $\bar{\theta}$, or the amount of water around a single root, decreases exponentially with time. We write the dimensionless amount of water uptake as

$$\phi = \frac{\bar{\theta}(0) - \bar{\theta}(\hat{t})}{\bar{\theta}(0)} = 1 - \exp(-\lambda_1^2\hat{t}) = 1 - \exp\left(-\frac{\lambda_1^2 D}{s^2}t\right). \tag{2.6}$$

Here, ϕ represents the fractional amount of water uptake to the available water content, often referred to as proportional water capture [30]. Using the relation between the root length density L_v and the half distance between adjacent roots s, $L_v = 1/(\pi s^2)$ (figure 1*c*), ϕ is reduced to $\phi = 1 - \exp(-\pi\lambda_1^2 D L_v t)$. ϕ at time $t = T$ is often expressed as

$$\phi = 1 - \exp(-kL_v), \tag{2.7}$$

where $k = \pi\lambda_1^2 DT \approx 18.2DT$ is referred to as the resource capture coefficient [30–33].

The resource capture coefficient, k, represents the ability of the root to capture water for T, a time interval for which a plant absorbs water while decreasing soil water content. The time interval T is typically defined as a half the duration between the maximum and minimum soil water content considering that root water uptake occurs in the daytime [34]. The lumped variable k includes the effects of the diameter and conductances of the root as well as properties of the surrounding soil.

Because we simplify a root system as a bundle of root fibres having a uniform diameter and assume k as a constant, it is the vertical distribution of root length density, $L_v(z)$, that determines water uptake as shown in equation (2.7). The exponential saturation of the water uptake in equation (2.7) suggests that an excessive increase in root length density in a soil layer yields only marginal gain in water uptake for a given time T. We define the proportional water capture of the entire root system with a depth of h as $\Phi = \int_0^h \phi\,dz$, which represents the volume of water uptake per unit area.

3. Optimization problem

3.1. Model description

An optimal length density distribution of a root system would maximize the total water uptake for a given cost. Thus we seek to find $L_v(z)$ that maximizes $\Phi = \int_0^h 1 - \exp(-kL_v)\,dz$ subject to a constraint related to the construction cost.

We first estimate the metabolic cost for a root system. During the root elongation, mechanical stress affects the elongation process in a complex manner. The increase in the force required to deform the soil not only suppresses the elongation directly but also perturbs the turgor pressure [35], the cell wall extensibility and yield threshold [36]. As a result, morphological [36] and metabolic [37] characteristics of roots change in response to the mechanical stress. The metabolic cost to form a root element by unit length is higher in the deeper soil layers because of the high mechanical stress [37]. As the mechanical stress of soil linearly increases with depth [38,39], we estimate the metabolic cost for a root system with L_v as

$$W = \int_0^h 2\pi a z L_v\,dz, \tag{3.1}$$

where a signifies the metabolic cost required for the root with

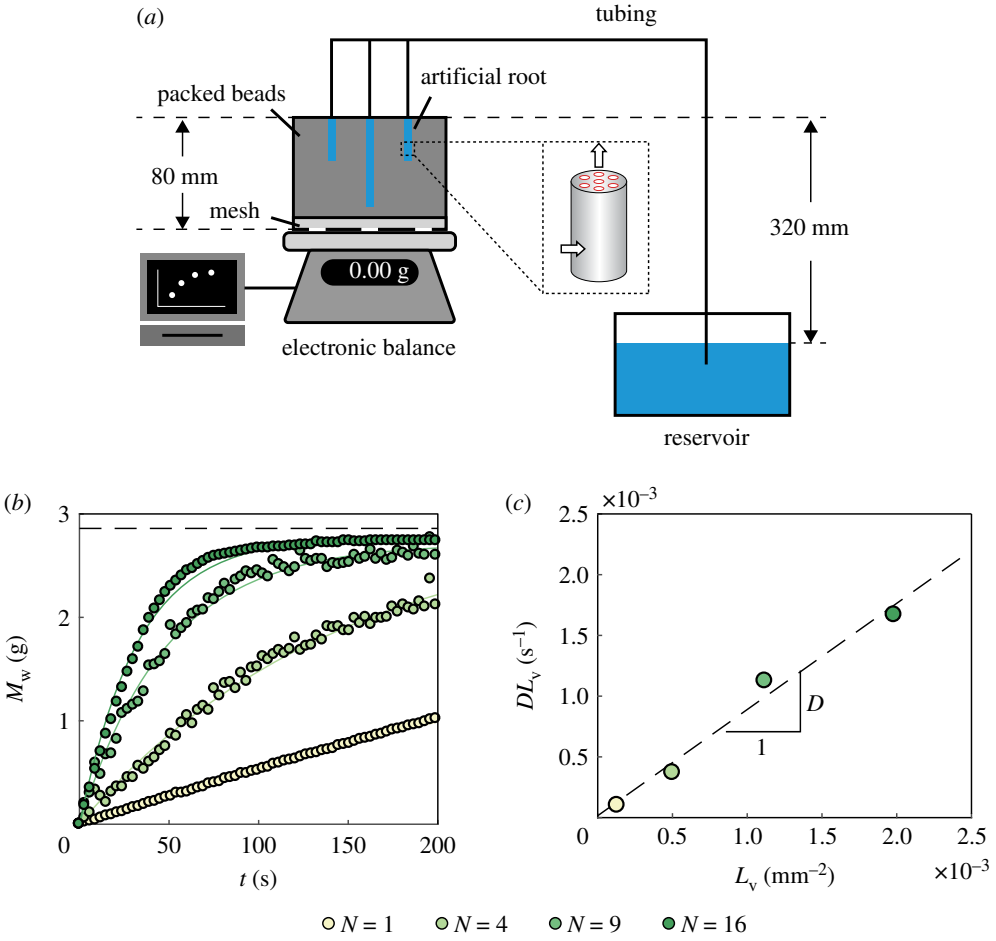

Figure 3. (*a*) Schematic illustration of the experimental set-up. The inner structure of the artificial root is shown in the dashed box. Water absorbed from the porous surrounding flows axially in the root through the seven internal conduits (red circles). (*b*) Temporal change of the absorbed water mass M_w for various numbers of root threads, $N = 1$, 4, 9 and 16. The curves represent the least-square fitting curves, $M_w = M_m[1 - \exp(-18.2D\,L_v t)]$. (*c*) The linear dependence of the values of measured DL_v on L_v. (Online version in colour.)

$L_v = 1/\pi$ to grow from the top soil layer of unit area to the unit depth. We note that a depends on frictional force of soil [38] and energetic costs of physiological processes affected by the mechanical stress of soil [35–37,40]. The depth z in the integrand corresponds to a weighting factor considering the increase of metabolic cost with depth.

We now seek a distribution of root length density that maximizes the proportional water capture Φ at a given cost budget W. By solving the optimization problem built upon the Euler–Lagrange equation, we obtain the optimal root length density as a function of depth

$$L_v(z) = -\frac{1}{k}\ln\frac{z}{h} \quad \text{for } 0 < z < h, \tag{3.2}$$

and $L_v(z)=0$ for $z \geq h$ by definition. Substituting equation (3.2) into equation (3.1) yields $h = \sqrt{2kW/(\pi a)}$.

It follows that the mean value of the optimal root length density, $\bar{L}_v = (1/h)\int_0^h L_v\,dz = 1/k$, revealing that $\bar{L}_v$ depends only on the resource capture coefficient k. This implies that the average root length density is determined solely by water capture rate of the root. Non-dimensionalization of equation (3.2) using the mean root length density leads to

$$L_v^* = -\ln z^*, \tag{3.3}$$

where $L_v^* = L_v/\bar{L}_v$ and $z^* = z/h$, implying that the distribution of the dimensionless root length density decays logarithmically with a scaled depth regardless of the factors determining the root water uptake and growth.

3.2. Verification of theory with biological data

We compare the distribution of dimensionless root length density of real plants with our theoretical prediction. Figure 2 shows that the extensive data collapse onto a single curve as predicted by equation (3.3) although the original raw data exhibit a large scatter in the inset. While those plants with fibrous root systems, wheat, maize, barley and fescue, follow the optimum curve well, the plants with tap root systems, soyabean and groundnut, slightly deviate from the optimum curve (deviation less than 5%, figure 2*b*). Although roots emerge from various root axes in the tap root system of legumes, they tend to grow vertically in parallel with uniform diameter, which corresponds to our simplification of root architecture. Hence, normalized root length density of soyabean is close to the optimum curve, equation (3.3), as shown in figure 2*b*.

4. Artificial root systems

4.1. Measurement of diffusivity

We further tested our theoretical model using the artificial roots embedded in packed glass beads as shown in figure 3*a* (see appendix A for detailed description). One

thread of artificial root consists of seven parallel cylindrical holes of 900 µm diameter surrounded by a nanofiltration layer of polyethersulfone (a dotted box in figure 3*a*). The threads were connected to the reservoir through flexible tubes to drain water from the bead packing to the reservoir as a siphon. We recorded the weight change of the bead container over time, which is equivalent to the water mass extracted from the bead packing.

To estimate the diffusivity of the bead packing, we first measured the water uptake rate by evenly distributed artificial roots that are identically 80 mm long, while changing the number of root threads (N) (figure 3*b*). The mass of extracted water follows $M_w(t) = M_m[1 - \exp(-18.2D\ L_v t)]$ as shown in equation (2.7). The number of the root threads divided by the cross-sectional area of the container is equivalent to the root length density, so that $L_v = (1.2,\ 4.9,\ 11 \text{ and } 20) \times 10^{-4}\ \text{mm}^{-2}$ for $N = 1,\ 4,\ 9$ and 16 in our experiments. The solid lines in figure 3*b* that best fit the experimental data in the form of $M_w(t) = M_m[1 - \exp(-18.2DL_v t)]$ allow us to obtain the diffusivity as $D = (1.08 \pm 0.11) \times 10^{-4}\ \text{mm}^2\ \text{s}^{-1}$ (estimated slope ± uncertainty, of the least-square fitting), as shown in figure 3*c*. Here, we took the maximum mass of extractable water in a layer, $M_m = M_w/\phi$ as 2.86 g, a value corresponding to the broken line in figure 3*b*. For the duration of our experiments, $T = 190$ s, k is given by $18.2DT = (3.73 \pm 0.38) \times 10^{-1}\ \text{mm}^2$.

4.2. Optimization in a finite number of soil layers

We consider a finite number of soil layers rather than the continuous ones for the design of artificial root systems. The discretized objective function and constraint are then given by

$$\Phi_d = \sum_{i=1}^{n} (1 - e^{-kL_{v,i}})\Delta z \tag{4.1}$$

and

$$\sum_{i=1}^{n} 2\pi a z_i L_{v,i} \Delta z = W_d, \tag{4.2}$$

where n is the number of soil layers, Δz is the thickness of each soil layer, z_i is the depth of ith layer and $L_{v,i}$ is the root length density in ith layer. Applying the method of Lagrange multipliers, we obtain the solution of the form similar to that of the continuous model, which is given by

$$L_{v,i} = -\frac{1}{k} \ln\left(\frac{\Delta z i}{h_d}\right), \tag{4.3}$$

where $h_d \approx \sqrt{2kW_d/(\pi a)}$ is the depth of an optimized artificial root system.

4.3. Optimal design for artificial roots

We now change the length distribution of the artificial root to see its effects on the water extraction rate. We tested four different distributions with the identical cost or depth-weighted root volume Ω, where $\Omega = \sum_{i=1}^{8} z_i L_{v,i} \Delta z$ with z_i, $L_{v,i}$, and Δz being the depth of ith layer, the root length density at ith depth, and the depth of a single layer (10 mm), respectively.

We designed four different distributions of artificial roots that have the same cost of construction. We regarded the entire domain as being composed of eight independent layers. We solved the discrete version of the optimization problem to

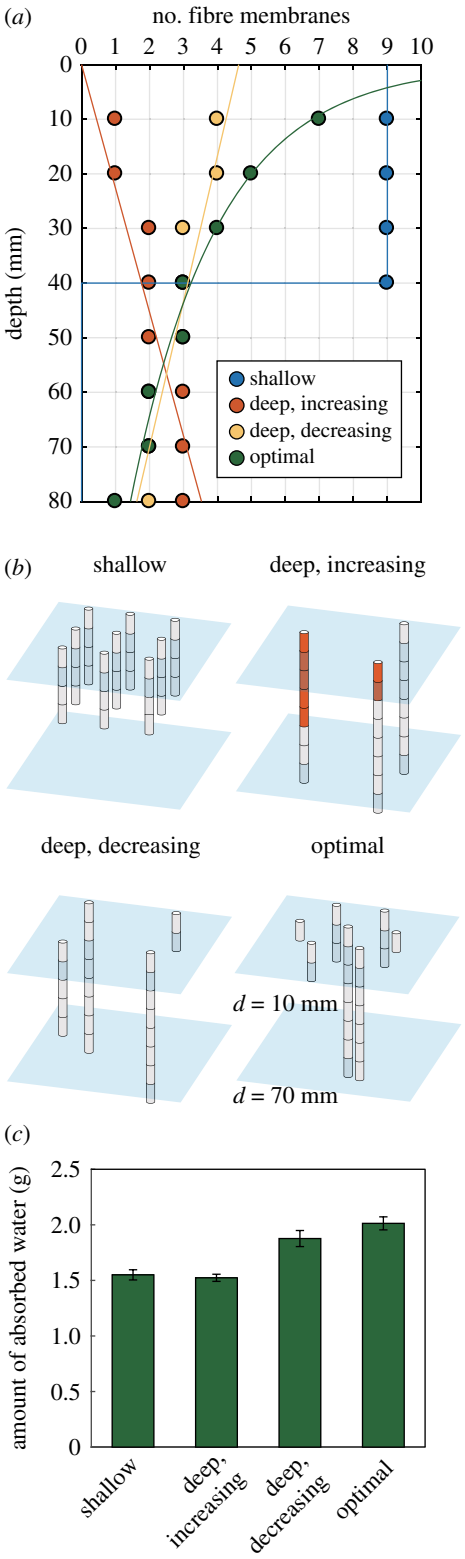

Figure 4. Designs of artificial roots. (*a*) The distribution of the artificial root units over depth. (*b*) Schematic of the different artificial root distributions. The red colour indicates the impermeable coat. (*c*) Comparison between the artificial root designs. The error bars represent the standard deviation of the measurements. (Online version in colour.)

find the optimal distribution of the artificial root system

$$\left.\begin{aligned} &\max_{L_v} && \Phi_d(L_v) = \sum_{i=1}^{8} (1 - e^{-kL_{v,i}})\Delta z \\ &\text{and} && \text{subject to} \quad \sum_{i=1}^{n} z_i L_{v,i} \Delta z = W_d,\ L_{v,i} \geq 0 \text{ for all } i, \end{aligned}\right\} \tag{4.4}$$

where $\boldsymbol{L}_v = (L_{v,1}, L_{v,2}, \ldots, L_{v,8})$, $k = (3.73 \pm 0.38) \times 10^{-1}$ mm^2, and the constant W_d is arbitrarily set to 9000 in order to generate distributions of experimental convenience. We found that the objective function under the constraint is maximized with $\boldsymbol{L}_{v,opt} = -(1/k)\ln((\Delta zi)/h_d)$ as predicted by equation (4.3). $\boldsymbol{L}_{v,opt}$ is approximately equal to $(7, 5, 4, 3, 3, 2, 2, 1) \times L_1$, where $L_1 = 1/90^2$ mm^{-2} is the root length density when a single thread is placed in a layer. The other equal-cost distributions are selected as

$$\left.\begin{aligned} \boldsymbol{L}_{v,1} &= (9, 9, 9, 9, 0, 0, 0, 0)L_1 \\ \boldsymbol{L}_{v,2} &= (4, 4, 3, 3, 3, 2, 2, 2)L_1 \end{aligned}\right\} \quad \text{and} \quad \left.\begin{aligned} \boldsymbol{L}_{v,3} &= (1, 1, 2, 2, 2, 3, 3, 3)L_1 \end{aligned}\right\} \tag{4.5}$$

where $\boldsymbol{L}_{v,1}$, $\boldsymbol{L}_{v,2}$ and $\boldsymbol{L}_{v,3}$ denote shallow, deep (decreasing) and deep (increasing) distribution, respectively (figure 4). Other possible combinations of root placement would yield different performances but not outperform the logarithmic distribution as the optimization problem implies.

Figure 4*c* compares the amount of absorbed water by the four root systems for 190 s. We see that the root system with logarithmically decreasing L_v absorbs more water than the other distributions. The linearly decreasing L_v exhibits the second-best performance. A root system of decreasing L_v with deep roots is generally advantageous because of the large water availability throughout the soil profile. Despite the deep roots, however, the root system with increasing L_v cannot fully capture the available water due to lack of root lengths. The distribution with abundant roots only in shallow layers is disadvantageous because the water availability is bounded in the limited region.

5. Conclusion

It has been reported that the vertical distribution of normalized root length density of crops can be described by a single mathematical curve [13,19]. Suggested functions that fit the observed data have provided us with various applications that require accurate information of root development and distribution [19,30,32]. Those empirical relations, however, are unable to explain why the relative distribution of various crop species converges to a single mathematical curve. Meanwhile, optimization models of the root have been proposed based on various cost and benefit functions [5–7,10,16,17], but they have lacked supporting data.

The present model considers the cost and benefit of root growth as simple mathematical functions while simplifying the plant- and environment-specific morphology and architecture. The spatio-temporal complexity of the soil environment on the cost is regarded insignificant compared to the effects of mechanical stress; for example, spatio-temporal change in soil temperature is usually well within the optimal condition for root growth [41,42]. On the other hand, mechanical stress in the soil more than 10 cm from the top overwhelms the cell wall yield threshold (0.3 MPa) [36].

We set an optimization problem to find root length density distribution maximizing benefit (Φ) given a cost budget (W) based on models concerning root water uptake and growth. The optimal distribution is obtained by applying the variational principle, which is frequently employed for the analysis of network systems in nature [43–45]. The solution, $L_v^* = -\ln z^*$, agrees well with the biological observation (figure 2*b*), and the experimental results using an artificial root system. Although the form of root network of mature plants is a cumulative result of the complex dynamics of growth under local environmental conditions as well as the genetics [2,3,46,47], our study explains the characteristics of root distribution of each species and suggests a rational pathway to understand botanical morphogenesis.

Our model reveals that deep root proliferation may not be cost-effective contrary to the common belief that plants with dense deep roots are advantageous for water capture. In the case of the transgenic groundnut shown in figure 2*b*, root length density severely deviates from the optimum curve, implying cost-inefficient water uptake by those transgenic crops. Although it was shown that they could extract more water than wild-types [1], their root systems are not necessarily efficient when considering the cost of root construction. Adapting crops to water stress via transgenic and/or breeding approaches has often overlooked overall effects of transgenic events including the metabolic costs [16] and hydraulic characteristics in plant scale [48]. Therefore, the degree of deviation from the optimal design derived from the model might be particularly useful for agricultural practice such as crop breeding to improve crops against water deficits.

In recent years, various plant-inspired systems have been designed and built to reproduce biological phenomena in the laboratory, which include transpiration [49,50], phloem loading [51] and cavitation in the xylem [52]. Our root-mimicking system enables us to control and observe the root water uptake, which might have potential as a testbed for artificial roots before actual crop breeding.

The design principle captured by the minimal model suggests a strategy to achieve cost-effective transport in multiscale porous media considering the cost as well as the performance. Reducing the resistance in deep soil, for example, by generating macropores [39], would lead to deep root proliferation and securing more water. One can consider manipulating the root genetically [1,4] so as to facilitate root elongation in mechanically stressed conditions. We also note that soilless cultivation, which is increasingly important in food production industry, now aims to tailor plants to maximize their yield [53]. Such technology can also benefit from our theoretical framework to seek optimal root length distribution with modified benefit and cost functions. In particular, the contribution of soil resistance in the cost function would be mitigated in soilless cultivation, requiring us to identify the pertinent costs for root growth whose candidates include metabolic cost of tissue growth and maintenance. Those efforts would allow for the innovation in agriculture against the intensive irrigation and help to resolve the global water and food crisis [48,54,55]. In addition, the design principle can lead to various cost-effective heat and mass transport systems in porous media [56].

Data accessibility. All data generated or analysed during this study are included in this published article and its electronic supplementary material.

Authors' contributions. K.H.J., W.K. and H.-Y.K. designed the research; Y.J. and K.P. performed research; Y.J., K.P., K.H.J., W.K., H.-Y.K. analysed the data and wrote the paper.

Competing interests. The authors declare no conflict of interest.

Funding. We thank University Farm of Seoul National University for providing the rice plant for photographing. H.-Y.K. was supported by the National Research Foundation of Korea (grant no. 2018052541) via S.N.U. I.A.M.D.. W.K. was supported by

the National Research Foundation of Korea (grant no. 2017R1E1A1A01073599).

Appendix A. Degree of deviation of root length density distribution from optimum

We suppose a distribution of normalized root length density in the form of $L^*_{v,n} = -n \ln z^*$, where n equals unity for optimal distribution and differs from unity for non-optimum. Given a construction cost W, maximum depth of the suboptimal root system, h, is given by $h = [2kW/(\pi an)]^{1/2}$ because $W = \int_0^h 2\pi a z L_{v,n}(z)\,dz = \pi a n h^2/(2k)$ where $L_{v,n} = -(n/k)\ln(z/h)$. In addition, the proportional water capture of a root system, Φ_n, is obtained as $\Phi_n = nh/(n+1)$ by substituting $L_{v,n} = -(n/k)\ln(z/h)$ into $\Phi_n = \int 1 - \exp(-kL_{v,n})\,dz$. Because $h \sim n^{-1/2}$, $\Phi_n \sim n^{1/2}/(n+1)$ and it has the global maximum at $n = 1$. The degree of deviation of root length density distribution from optimum, ϵ, is defined as the scaled difference of the amounts of water capture of optimum (Φ_1) and non-optimum (Φ_n), $\epsilon = (\Phi_1 - \Phi_n)/\Phi_1$, which is then given by

$$\epsilon = 1 - \frac{2n^{1/2}}{n+1}. \qquad \text{(A 1)}$$

Appendix B. Experiments using the artificial roots embedded in glass beads

An acrylic container with a size of 90 × 90 × 80 mm in length, width and height, respectively, was prepared. After drilling nine holes on the bottom of the container, we covered the bottom with a wired mesh. Quasi-monodisperse beads with a diameter range between 70 and 110 mm filled the container. Cylindrical artificial roots (Multibore 0.9 membrane, Inge GmbH) were bonded with 19 G syringe needles by an epoxy adhesive. The other end of the roots was blocked by applying the epoxy adhesive to guide only the side wall of the membrane to absorb water. The syringe needles were connected to a reservoir placed 320 mm below the top surface of the beads through the flexible polymer tubes with an inner diameter of 0.7 mm. Water was supplied on the top surface of the bead packing, and drained through the mesh on the holed bottom while tubes were blocked, which determined the initial water content in the bead packing. When the tubes opened, water in the bead packing was allowed to flow toward the reservoir. Weight change of the acrylic box being drained was recorded by an electronic scale (PAG4102, Ohaus).

Appendix C. References for root length density data of each plant species

Table 1. References for root length density data of each plant species.

species	reference
Triticum aestivum L.	[39,57–60]
Zea mays L.	[61,62]
Hordeum vulgare	[62,63]
Festuca arundinacea	[64,65]
Glycine max (L.) Merr.	[61,62]
Arachis hypogaea L.	[1]

References

1. Vadez V, Rao JS, Bhatnagar-Mathur P, Sharma KK. 2013 DREB1A promotes root development in deep soil layers and increases water extraction under water stress in groundnut. *Plant Biol.* **15**, 45–52. (doi:10.1111/j.1438-8677.2012.00588.x)
2. Dupuy LX, Mimault M, Patko D, Ladmiral V, Ameduri B, MacDonald MP, Ptashnyk M. 2018 Micromechanics of root development in soil. *Curr. Opin Genet. Dev.* **51**, 18–25. (doi:10.1016/j.gde.2018.03.007)
3. Robbins II NE, Dinneny JR. 2018 Growth is required for perception of water availability to pattern root branches in plants. *Proc. Natl Acad. Sci. USA* **115**, E822–E831. (doi:10.1073/pnas.1710709115)
4. Uga Y *et al.* 2013 Control of root system architecture by DEEPER ROOTING 1 increases rice yield under drought conditions. *Nat. Genet.* **45**, 1097–1102. (doi:10.1038/ng.2725)
5. Postma JA, Dathe A, Lynch JP. 2014 The optimal lateral root branching density for maize depends on nitrogen and phosphorus availability. *Plant Physiol.* **166**, 590–602. (doi:10.1104/pp.113.233916)
6. Fitter AH, Stickland TR, Harvey ML, Wilson GW. 1991 Architectural analysis of plant root systems 1. Architectural correlates of exploitation efficiency. *New Phytol.* **118**, 375–382. (doi:10.1111/j.1469-8137.1991.tb00018.x)
7. Landsberg JJ, Fowkes ND. 1978 Water movement through plant roots. *Ann. Bot.* **42**, 493–508. (doi:10.1093/oxfordjournals.aob.a085488)
8. Zwieniecki MA, Thompson MV, Holbrook NM. 2002 Understanding the hydraulics of porous pipes: tradeoffs between water uptake and root length utilization. *J. Plant Growth Regul.* **21**, 315–323. (doi:10.1007/s00344-003-0008-9)
9. Couvreur V, Faget M, Lobet G, Javaux M, Chaumont F, Draye X. 2018 Going with the flow: multiscale insights into the composite nature of water transport in roots. *Plant Physiol.* **178**, 1689–1703. (doi:10.1104/pp.18.01006)
10. Ho MD, McCannon BC, Lynch JP. 2004 Optimization modeling of plant root architecture for water and phosphorus acquisition. *J. Theor. Biol.* **226**, 331–340. (doi:10.1016/j.jtbi.2003.09.011)
11. Bejan A, Zane JP. 2012 *Design in nature: how the constructal law governs evolution in biology, physics, technology, and social organization*. New York, NY: Knopf Doubleday Publishing Group.
12. Bondy A, Murty USR. 2011 *Graph theory*. London, UK: Springer.
13. Gerwitz A, Page ER. 1974 An empirical mathematical model to describe plant root systems. *J. Appl. Ecol.* **11**, 773–781. (doi:10.2307/2402227)
14. Schenk HJ. 2008 The shallowest possible water extraction profile: a null model for global root distributions. *Vadose Zone J.* **7**, 1119–1124. (doi:10.2136/vzj2007.0119)
15. Lambers H, Atkin OK, Millenaar FF. 2002 17. *Respiratory patterns in roots in relation to their functioning*. New York, NY: Marcel Dekker.
16. Lynch JP. 2013 Steep, cheap and deep: an ideotype to optimize water and N acquisition by maize root systems. *Ann. Bot.* **112**, 347–357. (doi:10.1093/aob/mcs293)
17. Lynch JP. 2007 Rhizoeconomics: the roots of shoot growth limitations. *Hortscience* **42**, 1107–1109. (doi:10.21273/HORTSCI.42.5.1107)
18. Jackson RB, Canadell J, Ehleringer JR, Mooney HA, Sala OE, Schulze ED. 1996 A global analysis of root distributions for terrestrial biomes. *Oecologia* **108**, 389–411. (doi:10.1007/BF00333714)
19. Zuo Q, Jie F, Zhang R, Meng L. 2004 A generalized function of wheat's root length density distributions. *Vadose Zone J.* **3**, 271–277. (doi:10.2136/vzj2004.2710)

20. Hollister SJ. 2005 Porous scaffold design for tissue engineering. *Nat. Mater.* **4**, 518–524. (doi:10.1038/nmat1421)
21. Drury JL, Mooney DJ. 2003 Hydrogels for tissue engineering: scaffold design variables and applications. *Biomaterials* **24**, 4337–4351. (doi:10.1016/S0142-9612(03)00340-5)
22. Schüth F. 2005 Engineered porous catalytic materials. *Annu. Rev. Mater. Res.* **35**, 209–238. (doi:10.1146/annurev.matsci.35.012704.142050)
23. Parlett CMA, Wilson K, Lee AF. 2013 Hierarchical porous materials: catalytic applications. *Chem. Soc. Rev.* **42**, 3876–3893. (doi:10.1039/C2CS35378D)
24. Dawson R, Cooper AI, Adams DJ. 2012 Nanoporous organic polymer networks. *Prog. Polym. Sci.* **37**, 530–563. (doi:10.1016/j.progpolymsci.2011.09.002)
25. Svec F. 2010 Porous polymer monoliths: amazingly wide variety of techniques enabling their preparation. *J. Chromatogr. A* **1217**, 902–924. (doi:10.1016/j.chroma.2009.09.073)
26. Sadeghi A, Tonazzini A, Popova L, Mazzolai B. 2014 A novel growing device inspired by plant root soil penetration behaviors. *PLoS ONE* **9**, e90139. (doi:10.1371/journal.pone.0090139)
27. Sadeghi A, Mondini A, Mazzolai B. 2017 Toward self-growing soft robots inspired by plant roots and based on additive manufacturing technologies. *Soft Robot* **4**, 211–223. (doi:10.1089/soro.2016.0080)
28. Gregory PJ. 2006 Roots, rhizosphere and soil: the route to a better understanding of soil science? *Eur. J. Soil Sci.* **57**, 2–12. (doi:10.1111/j.1365-2389.2005.00778.x)
29. Tinker PB, Nye PH. 2000 *Solute movement in the Rhizosphere*. Oxford, UK: Oxford University Press.
30. King J, Gay A, Sylvester-Bradley R, Bingham I, Foulkes J, Gregory P, Robinson D. 2003 Modelling cereal root systems for water and nitrogen capture: towards an economic optimum. *Ann. Bot.* **91**, 383–390. (doi:10.1093/aob/mcg033)
31. Passioura JB. 1983 Roots and drought resistance. *Agric. Water Manage.* **7**, 265–280. (doi:10.1016/0378-3774(83)90089-6)
32. White CA, Sylvester-Bradley R, Berry PM. 2015 Root length densities of UK wheat and oilseed rape crops with implications for water capture and yield. *J. Exp. Bot.* **66**, 2293–2303. (doi:10.1093/jxb/erv077)
33. Monteith JL. 1986 How do crops manipulate water supply and demand? *Phil. Trans. R. Soc. Lond. A* **316**, 245–259. (doi:10.1098/rsta.1986.0007)
34. Ferchaud F, Vitte G, Bornet F, Strullu L, Mary B. 2015 Soil water uptake and root distribution of different perennial and annual bioenergy crops. *Plant Soil* **388**, 307–322. (doi:10.1007/s11104-014-2335-y)
35. Greacen EL, Oh JS. 1972 Physics of root growth. *Nature New Biol.* **235**, 24–25. (doi:10.1038/newbio235024a0)
36. Bengough AG, Bransby MF, Hans J, McKenna SJ, Roberts TJ, Valentine TA. 2006 Root responses to soil physical conditions; growth dynamics from field to cell. *J. Exp. Bot.* **57**, 437–447. (doi:10.1093/jxb/erj003)
37. Atwell BJ. 1990 The effect of soil compaction on wheat during early tillering: III. Fate of carbon transported to the roots. *New Phytol.* **115**, 43–49. (doi:10.1111/j.1469-8137.1990.tb00920.x)
38. Brzinski TA, Mayor P, Durian DJ. 2013 Depth-dependent resistance of granular media to vertical penetration. *Phys. Rev. Lett.* **111**, 168002. (doi:10.1103/PhysRevLett.111.168002)
39. Hodgkinson L, Dodd IC, Binley A, Ashton RW, White RP, Watts CW, Whalley WR. 2017 Root growth in field-grown winter wheat: some effects of soil conditions, season and genotype. *Eur. J. Agron.* **91**, 74–83. (doi:10.1016/j.eja.2017.09.014)
40. Bengough AG, Mullins CE. 1990 Mechanical impedance to root growth: a review of experimental techniques and root growth responses. *J. Soil Sci.* **41**, 341–358. (doi:10.1111/j.1365-2389.1990.tb00070.x)
41. McMichael BL, Burke JJ. 1998 Soil temperature and root growth. *HortScience* **33**, 947–951. (doi:10.21273/HORTSCI.33.6.947)
42. Kaspar TC, Bland WL. 1992 Soil temperature and root growth. *Soil Sci.* **154**, 290–299. (doi:10.1097/00010694-199210000-00005)
43. Ronellenfitsch H, Liesche J, Jensen KH, Michele Holbrook N, Schulz A, Katifori E. 2015 Scaling of phloem structure and optimality of photoassimilate transport in conifer needles. *Proc. R. Soc. B* **282**, 20141863. (doi:10.1098/rspb.2014.1863)
44. Drobnitch ST, Jensen KH, Prentice P, Pittermann J. 2015 Convergent evolution of vascular optimization in kelp (Laminariales). *Proc. R. Soc. B* **282**, 20151667. (doi:10.1098/rspb.2015.1667)
45. Zwieniecki MA, Stone HA, Leigh A, Boyce CK, Holbrook NM. 2006 Hydraulic design of pine needles: one-dimensional optimization for single-vein leaves. *Plant Cell Environ.* **29**, 803–809. (doi:10.1111/j.1365-3040.2005.01448.x)
46. Dupuy L, Gregory PJ, Bengough AG. 2010 Root growth models: towards a new generation of continuous approaches. *J. Exp. Bot.* **61**, 2131–2143. (doi:10.1093/jxb/erp389)
47. Bastian P, Chavarría-Krauser A, Engwer C, Jäger W, Marnach S, Ptashnyk M. 2008 Modelling *in vitro* growth of dense root networks. *J. Theor. Biol.* **254**, 99–109. (doi:10.1016/j.jtbi.2008.04.014)
48. Vadez V. 2014 Root hydraulics: the forgotten side of roots in drought adaptation. *Field Crops Res.* **165**, 15–24. (doi:10.1016/j.fcr.2014.03.017)
49. Wheeler TD, Stroock AD. 2008 The transpiration of water at negative pressures in a synthetic tree. *Nature* **455**, 208–212. (doi:10.1038/nature07226)
50. Noblin X, Mahadevan L, Coomaraswamy IA, Weitz DA, Holbrook NM, Zwieniecki MA. 2008 Optimal vein density in artificial and real leaves. *Proc. Natl Acad. Sci. USA* **105**, 9140–9144. (doi:10.1073/pnas.0709194105)
51. Comtet J, Jensen KH, Turgeon R, Stroock AD, Hosoi AE. 2017 Passive phloem loading and long-distance transport in a synthetic tree-on-a-chip. *Nat. Plants* **3**, 17032. (doi:10.1038/nplants.2017.32)
52. Vincent O, Marmottant P, Quinto-Su PA, Ohl CD. 2012 Birth and growth of cavitation bubbles within water under tension confined in a simple synthetic tree. *Phys. Rev. Lett.* **108**, 184502. (doi:10.1103/PhysRevLett.108.184502)
53. Raviv LJH M. 2019 *Soilless culture: theory and practice*. London, UK: Academic Press.
54. Davies WJ, Bennett MJ. 2015 Achieving more crop per drop. *Nat. Plants* **1**, 15118. (doi:10.1038/nplants.2015.118)
55. Bishopp A, Lynch JP. 2015 The hidden half of crop yields. *Nat. Plants* **1**, 15117. (doi:10.1038/nplants.2015.117)
56. Müllner T, Zankel A, Svec F, Tallarek U. 2014 Finite-size effects in the 3D reconstruction and morphological analysis of porous polymers. *Mater. Today* **17**, 404–411. (doi:10.1016/j.mattod.2014.07.003)
57. Liu L, Gan Y, Bueckert R, Van Rees K. 2011 Rooting systems of oilseed and pulse crops. II: Vertical distribution patterns across the soil profile. *Field Crops Res.* **122**, 248–255. (doi:10.1016/j.fcr.2011.04.003)
58. Tang C, Rengel Z, Diatloff E, Gazey C. 2003 Responses of wheat and barley to liming on a sandy soil with subsoil acidity. *Field Crops Res.* **80**, 235–244. (doi:10.1016/S0378-4290(02)00192-2)
59. Gregory PJ, McGowan M, Biscoe PV. 1978 Water relations of winter wheat: 2. Soil water relations. *J. Agric. Sci.* **91**, 103–116. (doi:10.1017/S0021859600056665)
60. Cutforth HW, Angadi SV, McConkey BG, Miller PR, Ulrich D, Gulden R, Volkmar KM, Entz MH, Brandt SA. 2013 Comparing rooting characteristics and soil water withdrawal patterns of wheat with alternative oilseed and pulse crops grown in the semiarid Canadian prairie. *Can. J. Soil Sci.* **93**, 147–160. (doi:10.4141/cjss2012-081)
61. Allmaras RR, Nelson WW, Voorhees WB. 1975 Soybean and corn rooting in Southwestern Minnesota: II. Root distributions and related water inflow. *Soil Sci. Soc. Am. J.* **39**, 771–777. (doi:10.2136/sssaj1975.03615995003900040046x)
62. Dwyer LM, Stewart DW, Balchin D. 1988 Rooting characteristics of corn, soybeans, and barley as a function of available water and soil physical characteristics. *Can. J. Soil Sci.* **68**, 121–132. (doi:10.4141/cjss88-011)
63. Gregory PJ. 1988 Root growth of chickpea, faba bean, lentil, and pea and effects of water and salt stresses. In *World crops: cool season food legumes* (ed. RJ Sommerfield), pp. 857–867. Dordrecht, Netherlands: Springer.
64. Durand JL, Gonzalez-Dugo V, Gastal F. 2010 How much do water deficits alter the nitrogen nutrition status of forage crops? *Nutr. Cycl. Agroecosyst.* **88**, 231–243. (doi:10.1007/s10705-009-9330-3)
65. Malcolm BJ, Cameron KC, Di HJ, Edwards GR, Moir JL. 2014 The effect of four different pasture species compositions on nitrate leaching losses under high N loading. *Soil Use Manage.* **30**, 58–68. (doi:10.1111/sum.12101)